Synergistic effects of tethered growth factors and adhesion ligands on DNA synthesis and function of primary hepatocytes cultured on soft synthetic hydrogels

Citation: Mehta, Geeta, Courtney M. Williams, Luis Alvarez, Martha Lesniewski, Roger D. Kamm, and Linda G. Griffith. "Synergistic Effects of Tethered Growth Factors and Adhesion Ligands on DNA Synthesis and Function of Primary Hepatocytes Cultured on Soft Synthetic Hydrogels." Biomaterials 31, no. 17 (June 2010): 4657–4671.

As Published: http://dx.doi.org/10.1016/j.biomaterials.2010.01.138

Publisher: Elsevier

Persistent URL: http://hdl.handle.net/1721.1/99187

Version: Author's final manuscript: final author's manuscript post peer review, without publisher's formatting or copy editing

Published in final edited form as:
Biomaterials. 2010 June ; 31(17): 4657–4671. doi:10.1016/j.biomaterials.2010.01.138.

Synergistic effects of tethered growth factors and adhesion ligands on DNA synthesis and function of primary hepatocytes cultured on soft synthetic hydrogels

Geeta Mehta[a,1], **Courtney M. Williams**[a,1], **Luis Alvarez**[a], **Martha Lesniewski**[b], **Roger D. Kamm**[a,c], and **Linda G. Griffith**[a,c,d,*]

[a]Department of Biological Engineering, Massachusetts Institute of Technology, 77 Massachusetts Avenue, 16-429, Cambridge, MA 02139, USA

[b]Department of Materials Science and Engineering, Georgia Institute of Technology, Atlanta, GA, USA

[c]Department of Mechanical Engineering, Massachusetts Institute of Technology, 77 Massachusetts Avenue, 16-429, Cambridge, MA 02139, USA

[d]Center for Gynepathology Research and Center for Environmental Health Sciences, Massachusetts Institute of Technology, 77 Massachusetts Avenue, 16-429, Cambridge, MA 02139, USA

Abstract

The composition, presentation, and spatial orientation of extracellular matrix molecules and growth factors are key regulators of cell behavior. Here, we used self-assembling peptide nanofiber gels as a modular scaffold to investigate how fibronectin-derived adhesion ligands and different modes of epidermal growth factor (EGF) presentation synergistically regulate multiple facets of primary rat hepatocyte behavior in the context of a soft gel. In the presence of soluble EGF, inclusion of dimeric RGD and the heparin binding domain from fibronectin (HB) increased hepatocyte aggregation, spreading, and metabolic function compared to unmodified gels or gels modified with a single motif, but unlike rigid substrates, gels failed to induce DNA synthesis. Tethered EGF dramatically stimulated cell aggregation and spreading under all adhesive ligand conditions and also preserved metabolic function. Surprisingly, tethered EGF elicited DNA synthesis on gels with RGD and HB. Phenotypic differences between soluble and tethered EGF stimulation of cells on peptide gels are correlated with differences in expression and phosphorylation the EGF receptor and its heterodimerization partner ErbB2, and activation of the downstream signaling node ERK1/2. These modular matrices reveal new facets of hepatocellular biology in culture and may be more broadly useful in culture of other soft tissues.

*Corresponding author. Department of Biological Engineering, Massachusetts Institute of Technology, 77 Massachusetts Avenue, 16-429, Cambridge, MA 02139, USA. Tel.: +1 617 253 0013; fax: +1 617 253 2400. griff@mit.edu (L.G. Griffith). .
[1]These authors contributed equally to this work.

Appendix. Supplementary data Supplementary data associated with this article can be found, in the online version, at doi:10.1016/j.biomaterials.2010.01.138.

Appendix Figures with essential colour discrimination. Certain figures in this article, in particular Figs. 1, 3 and 9 have parts that are difficult to interpret in black and white. The full colour images can be found in the online version, at doi:10.1016/j.biomaterials.2010.01.138.

Keywords

Self assembled peptide gel; Extracellular matrix; RGD cell binding domain; Heparin binding domain; Tethered growth factor

1. Introduction

Cells *in vivo* obtain cues from a complex microenvironment comprising the extracellular matrix (ECM), autocrine and paracrine growth factors, cytokines, and surrounding cells, the presentation of which are spatially and temporally specific and which collectively define unique micromechanical environments [1]. Synthetic matrices with tunable features are increasingly being used to probe the synergistic roles various cues play in governing cell behavior, but many such approaches employ chemistries that are not readily accessible to investigators in cell biology labs. Self-assembling peptide hydrogels, which have been applied to several tissue engineering applications [2–6], are attractive scaffolds for designing synthetic ECM for *in vitro* studies. The basic building blocks are commercially available and gels can be fabricated in a facile manner to achieve a range of mechanical properties and functionalities. The gels can be further customized in a modular fashion using standard peptide synthesis routes to achieve new functionalities. Our objective here was to exploit these features of self-assembling peptide gels to investigate how different modes of stimulation of epidermal growth factor receptor (EGFR) regulate hepatocellular behavior synergistically with adhesion receptors.

We are motivated by observations that hepatocytes undergo robust DNA synthesis and replication *in vivo* in a soft tissue environment to regenerate liver mass post-hepatectomy, in a manner that appears to depend on EGFR stimulation [7]. Primary male rat hepatocytes express abundant EGFR (>250,000 per cell) [8], which can bind both soluble and matrix-associated ligands, including EGF, TGF-α, and amphiregulin. *In vitro*, EGFR stimulation regulates hepatocyte attachment and survival during the initial stages of culture [8,9] and stimulates DNA synthesis in low density, highly adhesive cultures [10-13] via signaling pathways including MAPK/ERK, PLCγ, and PI3K/Akt. The phenotypic responses to EGFR stimulation may vary with different EGFR ligands due to differences in rates of internalization, trafficking, and recycling [14]. Interestingly, hepatocellular DNA synthesis *in vitro* generally requires a stiff substrate and low cell densities [13,15,16]. Peptide hydrogels offer a facile means to combine various adhesive and growth factor stimulation modes that mimic cues in the hepatic sinusoid, including the local mechanical properties, in a manner that may illuminate new facets of hepatocyte biology. We are particularly motivated to investigate how different mode of EGFR ligand presentation – soluble or tethered – influence hepatocellular responses *in vitro* because the hepatic sinusoid is known to contain tenascin-C [17], a matrix molecule with EGF-like repeats that activate EGFR in a matricrine manner [18]. Tethering of EGF to the synthetic ECM gel discourages internalization of ligand-bound EGFR and may alter the balance of the signaling pathways activated by EGFR [19] in ways that result in different phenotypes than stimulation with soluble EGF.

As a foundation for creating a synthetic gel microenvironment, we start with the commonly employed peptide gel backbone AcNRADARADARADARADA-CONH2 (RADA). RADA peptide gels do not contain any known adhesion motifs or ligands for other cell-surface receptors; however, functional motifs can be incorporated into the RADA backbone by direct peptide synthesis [20] and combined in various ratios with unmodified RADA peptide to form a gel with defined ligand density. Alternatively, incorporation of biotin onto the RADA backbone allows biotinylated growth factors to be attached to peptide gels through biotin–streptavidin linkage. The tethering of growth factors in other systems has been shown to

significantly alter their impact on cell behavior [8,19,21] and can control the spatial and temporal presentation of growth factors to inhibit receptor downregulation and alter the balance of signaling pathways [19]. Previously, a variety of adhesion motifs [20,22] and tethered insulin-like growth factor-1 (IGF-1) [2,6] have been used to functionalize the RADA peptide gel individually, but to our knowledge this is the first report on the use of peptide gels combining both adhesive modifications and a tethered growth factor. One point of particular interest in the hepatocyte cell culture system stimulated with EGFR ligands is that unlike the IGF receptor, the EGF receptor (EGFR) requires ligand-induced dimerization to initiate signaling. Primary hepatocytes express low or undetectable levels of the primary EGFR heterodimerization partner, ErbB2 [12], hence tethering of EGF to peptide gel represents a stringent system for analysis of the ability of peptide gels to present growth factor in a mode that leads to physiologically-relevant receptor activation for a receptor requiring dimerization.

In vivo, hepatocytes both make and bind to fibronectin via α5β1 and syndecan-4, hence we engineered adhesion by including the dimeric RGD motif PRGDSGYRGDS alone or together with the motif WQPPRARITGY (HB), the consensus heparin binding domain isolated from fibronectin which is known to bind the fibronectin co-receptor, syndecan-4 [23]. Together, RGD and HB approximate two co-operative signals required for cell adhesion to fibronectin [23].

Adhesion and growth factor stimuli regulate cell survival, proliferation, motility, and differentiation, and the response of cells to synthetic matrices may evolve in culture as autocrine factors secreted by cells (including matrix and matrix-binding growth factors) accumulate in the local extracellular environment. We therefore investigated the phenotypic response of hepatocytes to systematic variation of self assembled peptide gel stimuli using a panel of assays including immunohistochemistry, quantitative morphometry, and analysis of metabolism and protein secretion rates during 7 days of culture. Further we examined mechanistic links between stimuli and observed phenotypes by analyzing activity of intracellular signaling nodes associated with EGFR and integrin activation.

2. Materials and methods

2.1. Peptides and reagents

Commercially available self-assembling peptides were kindly provided by Dr. Lisa Spirio (3DM, Tokyo, Japan). Peptides in this category were: RADA-16-I (supplied as 1% w/v or 10 mg/mL; Ac-RADARADARADARADA-$CONH_2$) designated here as ‘RADA’; RGD-modified RADA [Ac-$(RADA)_4$-GPRGDSGYRGDS-$CONH_2$], designated here as ‘RGD2′, biotin-modified RADA [Ac-$(RADA)_4$-Biotin-$CONH_2$] designated here as ‘biotinylated RADA’. RADA modified with heparin binding domain of fibronectin [Ac-$(RADA)_4$-GGWQPPRARITGY-$CONH_2$], designated here as ‘HB’ was custom synthesized (CPC Scientific, San Jose, CA). All of the peptide gels made for this study included biotinylated RADA. The gel compositions and notation used in this report are shown in Table 1.

Human EGF suitable for incorporation into the peptide gel was produced as an engineered recombinant protein comprising the 53 amino acid human EGF domain fused to a protease-resistant 20 amino acid hydrophilic spacer arm [24], a single coil domain derived from a high-affinity coiled-coil pair [25,26], followed by a biotinylation sequence and epitope tag. The DNA sequence was ordered as a whole gene product with an *Escherichia coli* codon bias from GeneArt (Regensburg, Germany). Coding sequences were amplified by PCR mutagenesis with flanking restriction sites to permit cloning into pMALc2x expression vector (New England BioLabs). All expression constructs were sequenced prior to the transformation into the expression strain BL21(DE3)pLysS (Stratagene). Briefly, transformed strains were grown to OD ~ 0.6 with agitation at 37 °C. Cultures were brought to 25 °C and protein expression was

induced with a single pulse of 100 nM isopropyl β-D-1-thiogalactopyranoside (IPTG) for 4 h. Protein was harvested following cell lysis with Bug Buster Master Mix reagent (Novagen) supplemented with phenylmethylsulphonyl fluoride (PMSF) and protease inhibitor cocktail (Sigma). Lysates were clarified by centrifugation at 3500g for 1 h at 4 °C. Clear lysate was subjected to purification on amylose resin in accordance with the pMAL System protocol (New England BioLabs). Eluted protein was concentrated using an ultracentrifugation cassette (50 kDa molecular weight cut off, Pierce). Purification tags were cleaved by factor Xa digestion overnight at 30 °C in 20 mM tris, pH 7.4. Purity, quantity, and bioactivity were confirmed by SDS-PAGE, immunoblot, mass spectrometry, A280 (NanoDrop), and *in vitro* dose response vs. natural ligand wild type human EGF (Peprotech) in HeLa cells. Specificity for human EGFR activation was further assessed by including inhibitor controls using the pan-HER kinase inhibitor *N*-(4-((3-Chloro-4-fluorophenyl)amino)pyrido[3,4-d]pyrimidin-6-yl)2-butynamide (324840, Calbiochem). Biotinylation was carried out using biotin ligase (BirA) in accordance with vendor instructions (Avidity, Inc.). Extent of biotinylation was confirmed with a 4-hydroxyazobenzene-2-carboxylic acid (HABA) binding assay (Thermo Pierce). Extents of biotinylation of over 75% were typical of successful biotinylation reactions. The resulting EGF–biotin was tethered to RADA containing biotin by linkage through 0.2 mg/mL NeutrAvidin (31000, Thermo Fisher Scientific, Rockford, IL).

2.2. Gel formation

The peptide gel compositions and notation used in this report are shown in Table 1. Peptides were sonicated for at least 30 min before use (Aquasonic 50T, VWR Scientific). RADA and functional peptides (RGD2, HB, and biotinylated RADA) were mixed in the following ratios: 9:1 for RADA + biotinylated RADA; 8:1:1 for RADA + RGD2 + biotinylated RADA and 7:1:1:1 for RADA + RGD2 + HB + biotinylated RADA. Biotinylated RADA was included as a component in all gels to control for possible alterations in physicochemical properties of gels, including alterations in bulk mechanical properties [20]. The peptide gels were made in either 12- or 24-well transwell inserts (pore size = 0.4 μm) in 12 or 24 well plates. After sonication, 50 μL (for 12-well) or 70 μL (for 24-well) of peptide mixture was added to the transwell insert and lowered in a well with either 750 μL or 1 mL of hepatocyte growth media, incubated for 30 min and UV sterilized before use. For making tethered EGF peptide gels (tEGF gels), the transwell inserts containing peptide gels were washed with PBS after gelation and incubated with neutravidin (0.2 mg/mL) for 30 min. The neutravidin-linked samples were washed three times with PBS and incubated with EGF–biotin (0.71 μM) for 30 min. The resulting tEGF samples were washed three times with PBS and UV sterilized before use. Biotinylated growth factor bound to RADA peptide gels in this fashion have previously been shown to remain gel-associated for weeks [2,6].

2.3. Primary hepatocyte isolation

Primary cells were isolated from male Fisher rats weighing between 150 and 250 g as previously described [27] using Blendzyme III (Roche) in place of collagenase. Following isolation, cells were resuspended in DAG (Dulbecco's Modified Eagle's Medium (DMEM) with 2 g/L bovine serum albumin (BSA) and 50 mg/L gentamicin) and centrifuged, twice consecutively, at 50 g for 3 min, resulting in a hepatocyte-rich fraction. Using a ViCell counter with trypan blue exclusion, final cell viability was determined to range from 90 to 95% with a cell density between 8 and 13 million cells per milliliter.

2.4. Culture of primary hepatocytes on peptide gels

Following isolation, primary hepatocytes were resuspended in serum-free hepatocyte growth medium (HGM; low glucose DMEM supplemented with 4 mg/L insulin, 0.1 μM dexamethasone, 0.03 g/L proline, 0.1 g/L L-ornithine, 0.305 g/L niacinamide, 2 g/L D-(+)-

galactose, 2 g/L D-(+)-glucose, 1 mM L-glutamine, 50 mg/L gentamicin, 54.4 μg/L $ZnCl_2$,75 μg/L $ZnSO_4 \cdot 7H_2O$, 20 μg/L $CuSO_4 \cdot 5H_2O$, 25 μg/L $MnSO_4$) with or without 10 ng/mL EGF as indicated. Cells were plated on peptide gels at a density of 100,000 cells/cm^2 (for spreading or signaling assays) or 65,000 cells/ cm^2 (for viability or DNA synthesis assays) in either 24- or 12-well transwell inserts. HGM was replaced after 24 h and again every fourth day of culture. Cells were incubated at 37 °C, 5% CO_2 and 95% humidity for the time periods indicated EGF was included in cultures as indicated. Transwell inserts adsorbed with collagen I (BioCoat, BD Biosciences) were used as controls in some experiments.

2.5. Immunofluorescence microscopy

Samples were fixed in 3.7% formaldehyde in phosphate buffered saline (PBS) for 25 min at room temperature, permeabilized with 1% Triton-X for 10 min at 4 °C and washed with two changes of PBS for 15 min each. Samples were blocked for 1 h with 10% normal goat serum (Invitrogen) and 1% BSA in PBS. Samples were incubated with primary antibodies overnight at 4 °C and washed with 3 changes of PBS for 20 min each. Samples were then incubated with secondary antibodies, Alexafluor 568-phalloidin, and nuclear stain for 1 h at room temperature, protected from light, before being washed with 3 changes of PBS for 20 min each. Samples were then stored in PBS at 4 °C, protected from light. Visualization was done using a Zeiss Observer A1 microscope equipped with a Photometrics Quant EM S12SC camera and BD CARV II spinning disc confocal (Biovision Technologies). Images were acquired using MetaMorph software.

For DNA synthesis assays, after 24, 48 or 72 h in culture, medium was changed to HGM containing 10 μM of 5-Bromo-2′-Deoxyuridine (BrdU) (B9285, Sigma) to label DNA synthesizing hepatocytes on peptide gels for 24–48, 48–72 and 72–96 h. After 48, 72 or 96 h, the experiment was terminated and the incorporation of the BrdU was determined by immunofluorescence. The samples were fixed, permeabilized and treated with 2 M HCl for 20 min. Acid was removed and samples were washed with PBS containing 0.15% glycine and 0.5% BSA until pH returned to 7. Samples were blocked and stained for primary and secondary antibodies using routine protocol. Additionally, presence of nuclear antigen Ki67 at these time-points (48, 72 or 96 h) was also observed by immunofluorescence.

Primary antibodies include anti-rat fibronectin at 1:100 (Millipore), anti-rabbit Ki67 at 1:100 (Abcam), anti-mouse BrdU at 1:200 (Invitrogen). Secondary antibodies at 1:200 and phalloidin dyes at 1:200 were all AlexaFluor conjugates (Invitrogen). Nuclear stains were used at 1 μg/mL for 4′,6-diamidino-2-phenylindole (DAPI) (Sigma) and 16.2 mM for Hoechst 33342 (Invitrogen).

2.6. Cell number and viability measurement

Enumeration of live and dead cells was performed using live/dead viability kit (L3224, Invitrogen) to fluorescently label dead cells with ethidium bromide (EtBr) and all nuclei with DAPI. In each well, four to six randomly-chosen fields (one from each quadrant of the well) were observed using a 10 × objective, and all nuclei were counted in each field (300–600 total nuclei per field). The experiment was performed at least three times. The data were statistically analyzed with ANOVA followed by Tukey's test with alpha = 0.05.

2.7. Quantification of urea and albumin production

Culture medium was replaced 48 h prior to collection on the indicated days. Albumin concentrations were determined using rat albumin ELISA Kit (Bethyl Labs). Urea concentrations were determined using the QuantiChrom Urea Assay Kit (BioAssay Systems). Samples, standards and controls were tested in duplicates and experiments were repeated three to six times. In order to compare with previously published reports, in Figure S2, results are

reported as μg Product/μg DNA, where μg DNA was estimated using the initial cell number plated corrected according to viability data and assuming that 1×10^6 cells yields 4 μg DNA (as reported by Gibco for Trizol Reagent). The data were statistically analyzed with ANOVA followed by Tukey's test with alpha = 0.05.

2.8. Quantification of average projected cell aggregate area

Average cell area was quantified as total aggregate area (from phalloidin stained images) divided by total number of nuclei (from DAPI images) on Metamorph. Four to six individual images in phalloidin and DAPI channels of each sample were used for each measurement (200–600 nuclei per measurement). Phalloidin images were used for estimating projected area of cell aggregates by highlighting the cytoskeleton. Total cell number in the aggregates was obtained by counting DAPI-stained nuclei. The measurements were performed for four time-points: 4 h, 24 h, 3 days and 7 days. The experiments were repeated 3–4 times for statistical significance. The data were statistically analyzed with ANOVA followed with Tukey's test by alpha = 0.05.

2.9. Quantification of DNA synthesis

Fluorescent images of DAPI, BrdU and Ki67 staining were used for quantification of hepatocyte DNA synthesis by Image J. For BrdU images, the fluorescence intensities of the nuclei were also quantified to account for the variations in the size of the nuclei influencing signal intensity. The data were statistically analyzed with ANOVA followed with Tukey's test by alpha = 0.05.

2.10. Immunoprecipitation

To obtain cell lysates, samples were washed twice with ice cold PBS and lysed in RIPA buffer (Upstate Biotechnology, Waltham, MA) with protease inhibitors cocktail (Roche, Indianapolis, IN). Gels and cells collected were incubated on ice and passed through 26 gauge syringes. Lysates were microfuged at 16,000g for 15 min and supernatant collected. Immunoblotting was performed by normalizing cell lysates to GAPDH loading controls. Blots were transferred to nitrocellulose and probed with corresponding primary antibodies (9106 pERK, Cell Signaling) and secondary IR-Dye conjugate antibodies (IR-Dye700/800, Rockland). Membranes were scanned using a Licor Odyssey IR scanner (Licor Systems, Inc.). The data were statistically analyzed with ANOVA and Tukey's test by alpha = 0.05.

Novagen® bead kits were used for phosphorylated (pTyr) and total EGFR and ErbB2 (EMD Sciences) and pERK1/2 (BioRad). Ten μg of protein lysates from each sample were incubated overnight in filter plates (Millipore) with the appropriate antibody-bead conjugates. Unbound proteins were washed away by vacuum filtration of the plate, trapping the beads in the well. Beads were rinsed with vendor-supplied buffers and incubated with a biotinylated antibody specific for a second epitope on the target. Beads were rinsed again and incubated with streptavidin phycoerythin (Strep-PE), fluorescently tagging the antibody bound to the second epitope. Total EGFR and ErbB2 fluorescence was normalized to a standard curve generated with increasing concentrations of the extracellular domain of EGFR and HER2 provided by the manufacturer (Novagen). The data were statistically analyzed with ANOVA and Tukey's test by alpha = 0.05.

3. Results

3.1. Quantitative morphogenesis of multicellular aggregates

The balance of cell–cell and cell–matrix interactions governs the evolution of hepatocyte aggregate formation and hepatocellular aggregate morphogenesis in culture. Hepatocytes

plated onto minimally adhesive substrata form attached spherical aggregates within four days of plating, while cells on moderately- or highly adhesive substrata undergo aggregation while remaining highly spread [9]. Fibronectin is abundant in the extracellular environment of the hepatocyte *in vivo*, and supports attachment and spreading of hepatocytes *in vitro* [28–30]. Hepatocellular adhesion is also regulated by growth factor receptors such as EGFR. EGFR stimulation can promote cytoskeletal contraction and cleavage of cell-substrate bonds through activation of calpain [31], thus, it can also inhibit adhesion, as has been observed for hepatocytes andother cells seeded on moderately adhesive surfaces in the presence of soluble EGF [8]. Further, tethered EGFR ligands can elicit dramatically different responses than soluble ligands in some cell contexts [19], although previous studies in which tethered EGF was compared to soluble EGF in stimulating hepatocyte spreading and DNA synthesis showed comparable outcomes for both modes of presentation [8]. We sought here to determine whether hepatocytes would respond to tethered EGF differentially compared to soluble EGF in a physiologically-relevant matrix environment (soft hydrogel). We also sought to determine the effects of RGD2 and HB motifs, targeting adhesion through both integrin (RGD2) and syndecan-4 (HB), on cell and aggregate morphology.

The morphology of primary rat hepatocytes on peptide hydro-gels was observed at 4 and 24 h, 3 and 7 days. Hepatocytes attached and spread to form monolayer clusters or aggregates on all peptide gel formulations; however, the overall area of aggregates, as well as the average cell area within an aggregate, significantly increased upon inclusion of adhesion ligands and growth factor modifications. On functionalized peptide gels, even as early as 4 h after plating, hepatocytes have discernibly higher cortical actin and elongation of the cell body, as observed in the Alexafluor 568-phalloidin stained images (Supplemental data, Figure S1). The most striking difference in hepatocyte morphology (aggregate size and area per cell) as a function of the peptide gel composition was observed on day 3 as shown in Fig. 1A. With inclusion of RGD2 motifs, the cell aggregate areas increase; this effect is further enhanced by inclusion of HB with RGD2. Surprisingly, in gels that lack the HB domain, soluble and tethered EGF exert dramatically different effects on cell and aggregate morphology. In contrast to soluble EGF, which is associated with small aggregates, tethered EGF drives formation of large aggregates with relatively well-spread cells (Fig. 1A). In order to determine the impact on individual cell spreading, the average aggregate area and average area of each cell were calculated from the total aggregate area and the number of nuclei within each aggregate (Fig. 1B and C).

On RADA gels on day 3, hepatocytes exposed to soluble EGF exhibited an average cell area of 850 μm^2 – comparable to the projected area of a spherical hepatocyte – and average aggregate size was relatively small (6760 μm^2, Fig. 1C). However, hepatocytes exposed to tethered EGF on the RADA gel resulted in aggregates almost 20-fold larger (121,000 μm^2) with 1.3-fold greater spread areas per cell (1080 μm^2). Inclusion of the dimeric RGD2 domain (RADA + RGD2) in gels without tethered EGF increased the aggregate area by 6-fold (to 43,100 μm^2) and the per cell area by 1.2-fold (to 1040 μm^2) and addition of both the dimeric RGD2 domain and the heparin binding domain (RADA + RGD2 + HB)increased average aggregate area yet 9-fold further (to 388,000 μm^2) and likewise the cell spread area by another ~40% (to 1440 μm^2) in comparison to RADA with soluble EGF. Addition of tethered EGF to these adhesion ligand-modified peptide gels lead to a further increase in the hepatocyte cell and aggregate area at day 3. With just the RGD2 ligand, tethered EGF increased aggregate area 12-fold (to 525,000 μm^2) and cell area 1.6-fold (to 1730 μm^2). Inclusion of tethered EGF in gels with both the RGD2 and HB domains increased aggregate area 1.6-fold and average cell area 1.4-fold (to 1950 μm^2) over values for cells on the same gels in the presence of soluble (but not tethered) EGF.

3.2. Synergistic effects of adhesion peptides and EGF on hepatocyte viability

Hepatocyte survival in culture is influenced by cell–matrix adhesion and growth factor stimulation [9,10,27,32]. EGF can act as both a pro-survival signal and as a pro-death signal depending on the context [27]. In the absence of exogenous EGF (either tethered or soluble), hepatocytes on peptide gels show very low viability (20–50%) at day 3 that decreases over time in culture (data not shown). To determine whether the adhesive and growth factor modifications differed in their ability to support hepatocyte viability, we stained the nuclei of cells cultured in the presence of various combinations of adhesion ligands and growth factors with ethidium bromide (to label dead cells) and DAPI (to label all cells) and quantified the number of each in multiple representative fields for each condition (Fig. 2). Although plating efficiency was high for all conditions (Fig. 2B), cell numbers slightly declined for gels with the least adhesive phenotype (RADA) but increased for cells on the most adhesive phenotype (RADA + RGD2 + HB + tEGF) The decline in cell number was associated with lower viability in the early cell number stages of culture (Fig. 2A).

Peptide gels with RGD2 + HB + tEGF supported survival of hepatocytes at a greater level than peptide gels with no modifications at all time-points. After 24 h and 3 days, hepatocytes on RADA + RGD2, RADA + RGD2 + HB, RADA + RGD2 + tEGF, RADA + RGD2 + HB + tEGF had significantly higher viability than on RADA alone. However, by day 7, only hepatocytes on RADA + RGD2 + HB + tEGF had a significantly higher viability than on RADA alone. By seven days, the viability of hepatocytes was similar on most peptide gels, which may be the result of cell-secreted matrix accumulation. The apparent increase in viability of hepatocytes on peptide gels is due to gradual loss of dead cells by detachment during media changes, phagocytosis, or disintegration following apoptosis. These results are consistent with previous work demonstrating the importance of cell–matrix adhesion for growth factor signaling and the combination of both cues to cell survival [33]. Tethered EGF has a much stronger positive impact on hepatocyte survival on peptide gels than soluble EGF, a phenomenon that may arise from either sustained signaling by surface-restricted EGFR, or alteration of the balance of EGFR-mediated pathways toward pro-survival pathways including PI3 kinase/AKT.

3.3. Accumulation and assembly of cell-secreted fibronectin

Fibronectin is abundant in the liver sinusoids where hepatocytes produce plasma fibronectin for the blood supply of the entire organism [34]. Hepatocyte-produced fibronectin is in close contact with the cell-surface, and hepatocytes express the fibronectin binding integrin α5β1 and fibronectin co-receptor syndecan-4. To determine if hepatocytes on peptide gels produced and accumulated fibronectin, we used immunofluorescence microscopy to observe extracellular (fibrillar and non-fibrillar) and intracellular fibronectin produced by hepatocytes (Fig. 3). Overall, hepatocytes on unmodified gels showed little accumulation of fibronectin, while inclusion of RGD2, HB, and tethered growth factor modifications increased amounts of intracellular, soluble and fibrillar fibronectin at days 3 and 7.

On RADA peptide gels with soluble EGF, there was no fibronectin fibril assembly but weak staining of soluble (non-fibrillar) fibronectin observed on the surface of the peptide gels. Addition of RGD2 to RADA with soluble EGF increased the amount of nonfibrillar fibronectin. On inclusion of RGD2 and HB into peptide gels with soluble EGF, fibronectin fibrils (arrowheads) were observed on the gel surface. Moreover, with this gel configuration (RADA + RGD2 + HB), intracellular fibronectin (arrows) was also observed. No detectable fluorescence was seen when RADA + RGD2 gels without cells were incubated with anti-fibronectin antibody (data not shown).

Addition of tethered EGF to RADA increased the soluble staining for fibronectin on the peptide gel surface. On peptide gels containing either RGD2 or RGD2 + HB, the presence of tethered EGF led to increases in the intracellular and soluble fibronectin as well asassembly of fibronectin fibrils. In contrast to fibronectin assembly at day 3, as summarized above, immunofluorescence for fibronectin on peptide gels fixed at either 4 or 24 h showed little presence of fibronectin (data not shown). However at day 7, there was much more intracellular, soluble and fibrillar fibronectin on RADA + RGD2 + HB + tEGF peptide gels (data not shown) mirroring the same trend with respect to the peptide gel composition as on day3.

3.4. Hepatocyte DNA synthesis

While the liver can regenerate *in vivo*, *in vitro* it is difficult to get primary hepatocytes to enter into the cell cycle. Previous work has shown insulin and EGF (or TGF-α) stimulation *in vitro* prompts entry of primary adult hepatocytes into the cell cycle and synthesis of DNA, after a lag of 40 h, peaking between 48 and 72 h on collagen I coated tissue culture plastics [35]. However, matrices known to be similar in stiffness to liver tissue have been shown to inhibit that response [15]. In order to test the capacity of different compositions of peptide gels to support hepatocyte entry into the cell cycle Ki-67 staining was used to label cells in the active phases of the cell cycle (G1, S, G2, M) and DNA synthesis was quantified by BrdU incorporation. We quantified DNA synthesis via immunofluorescence staining as the percentage of total nuclei incorporating BrdU (within 24–48, 48–72 or 72–96 h) or as the percentage of total nuclei staining positive for Ki67 (at 48, 72 or 96 h) (Fig. 4). The presence of tethered EGF, RGD2, and HB were found to be critical for primary rat hepatocytes to synthesize DNA on peptide gels.

Remarkably, of the time-points and compositions tested, EGF-mediated DNA synthesis was only observed on peptide gels with RGD2, HB and tEGF modifications during the 48–72 h period of culture. We observed no DNA synthesis on any other peptide gel (RADA, RADA + RGD2, RADA + RGD2 + HB) even in the presence of soluble EGF. However, on adsorbed collagen type I in the presence of soluble EGF, we observed DNA synthesis via incorporation of BrdU and presence of Ki67 nuclear antigen at all time-points (40% BrdU incorporation in 24–48 h, 49% in 48–72 h, 44% in 72–96 h, and 28% Ki67 positive cells at 48 h, 35% at 72 h, 30% at 96 h). To compare, hepatocytes on RADA + RGD2 + HB + tEGF gels between 48 and 72 h showed 41% BrdU incorporation and 32% Ki67 positive cells. There is an expected difference between BrdU-positive cells and Ki-67-positive cells because BrdU incorporation was done over a 24-h period (ie. 24–48, 48–72 and 72–96 h) while the presence of Ki67 was detected only at the time of fixation.

These results are particularly interesting given that soft substrates of any composition are typically less supportive of hepatocyte entry into the cell cycle; in the presence of soluble EGF, DNA synthesis on a soft collagen I gel is only ~30% of that on adsorbed collagen I [15]. However, DNA synthesis rates on RADA + RGD2 + HB + tEGF peptide gels are similar to those on adsorbed collagen I with soluble EGF between 48 and 72 h. This suggests that the RADA + RGD2+HB + tEGF peptide gel captures certain aspects of the hepatocyte environment *in vivo*, where DNA synthesis proceeds in a soft mechanical environment.

3.5. Activation of fibronectin- and EGFR-mediated intracellular signaling pathways

Since integrins and growth factors are each known to trigger activation of the extracellular signal-regulated kinase (ERK) class of mitogen activated protein (MAP) kinases, we examined ERK activation as a pathway potentially involved in mediating the phenotypic differences seen on the various peptide gels. We monitored the presence of total and phosphorylated ERK (1 and 2), EGFR and ErbB2, the primary heterodimerization partner of EGFR, in primary cultures of rat hepatocytes on peptide gels. Tethered EGF induced higher levels of activation of EGFR

and ERK1/2 on various peptide gel compositions at later time-points compared to soluble EGF. Early (30 min) and sustained (24, 48 and 72 h) levels of ERK phosphorylation on peptide gels with either tethered or soluble EGF were quantified and data for later time-points are shown in Fig. 5.

Comparison of peptide gels with or without RGD2 at 30 min and 24 h yields similar ERK phosphorylation with soluble or tethered EGF (data not shown). However, at 48 and 72 h, on RADA, RADA + RGD2 and RADA + RGD2 + HB peptide gels, tethered EGF induced statistically higher ERK activation than soluble EGF. While there were striking differences with the various combinations of adhesive ligands in terms of cell spreading, viability, and metabolic function, there were no discernable differences between ERK phosphorylation at any of the time-points among any of the adhesion ligands; the only significant change in ERK1/2 phosphorylation arose from differences in the mode of EGFR stimulation (soluble vstethered EGF). This result was not unexpected, despite the robust phenotypic differences seen with the inclusion of adhesive modifications, as it has previously been reported that ERK signaling goes down after an initial period of attachment and spreading [36].It is also possible that robust signaling downstream of EGFR is obscuring signaling downstream of integrins.

In many cell types, activation of ERK1/2 by EGFR can be modulated by heterodimerization with the EGFR family member ErbB2. Although ErbB2 is normally expressed at low or undetectable levels in hepatocytes *in vivo*, its expression and activation status is induced in culture and is modulated by growth factors and hormones [12]. Hence, we examined the expression and phosphorylation of both EGFR and ErbB2 in primary rat hepatocytes cultured on different gel compositions. While inclusion of adhesion ligands (RGD2 and RGD2 + HB) increased EGFR phosphorylation in the presence of soluble EGF over levels observed on unmodified RADA at 72 h (Fig. 6B), the inclusion of adhesion ligands had little impact on the phosphorylation of the EGFR at the time-points examined. However, tethering of EGF had a dramatic impact on the total receptor levels and their phosphorylation at 48 and 72 h (Figs. 6A, B and 7A, B). EGFR phosphorylation (normalized to total EGFR and GAPDH) on all tethered EGF peptide gels was statistically higher than on their soluble EGF counterparts. ErbB2 phosphorylation showed the opposite pattern: ErbB2 phosphorylation (normalized to total ErbB2 and GAPDH) at 48 and 72 h was statistically lower on peptide gels with tethered EGF compared to their soluble EGF counterparts (Fig. 6C and D). Thus, the data indicate that EGFR is more extensively phosphorylated in the presence of tethered EGF, while ErbB2 is more extensively phosphorylated in the presence of soluble EGF.

Examination of total receptor levels, over time and in relation to freshly isolated hepatocytes, shows that in the presence of soluble EGF, EGFR levels decrease (Fig. 7A and B) while levels of ErbB2 increase (Fig. 7C and D). However, on peptide gels with tethered EGF, EGFR and ErbB2 levels both remain stable over time and when compared to fresh isolates, with EGFR levels being higher than ErbB2 levels (Fig. 7A–D). Previous reports have indicated that tethering of EGF can inhibit degradation of EGFR [19], which we observe here. However, others have shown that culturing hepatocytes in vitro leads to an up-regulation of ErbB2, typically not found on hepatocytes in vivo [12,37]. The ability of tethered EGF peptide gels to minimize or prevent up-regulation of ErbB2 may be further indication that this system captures cues that are critical to maintenance of hepatocyte differentiation. Further, these differences in EGFR and ErbB2 phosphorylation and dynamics between soluble and tethered EGF have not been previously reported and present an interesting avenue of future inquiry.

The similarity in the phosphorylation patterns of ERK1/2 and EGFR supports the conclusion that the absence of an adhesion-mediated phosphorylation difference is the result of strong signaling downstream of the growth factor receptor obscuring differences downstream of integrins. The data on ERK and EGFR activation are consistent with previous observations

with different cell types plated on surfaces with tethered EGF [19]. Thus, tethering EGF on peptide gels likely permits sustained EGF signaling since EGFR binding to tethered EGF inhibits endocytosis and degradation. This sustained EGF signaling may also explain the differences in viability between peptide gels with either soluble or tethered EGF ligands.

3.6. Coregulation of hepatocellular metabolic function by fibronectin peptides and tEGF

Hepatocytes perform numerous metabolic, endocrine and secretory functions in the liver, including synthesis of lipids, proteins and carbohydrates. However, primary hepatocytes typically show a dramatic decrease in these metabolic functions in vitro in standard culture conditions [38]. Here, we examined two of the critical metabolic functions of adult hepatocytes that are rapidly lost under standard cell culture conditions: urea production and albumin secretion. Addition of adhesive fibronectin moieties in conjunction with tethered growth factors dramatically improved the ability of hepatocytes to maintain these metabolic functions. Peptide gels with RADA + RGD2 + HB + tEGF supported the highest levels of urea and albumin production by hepatocytes at all time-points, providing a statistically significant increase over standard adsorbed collagen I culture conditions. Fig. 8 shows the urea (8A) and albumin (8B) produced by hepatocytes as a function of time on either peptide gels or adsorbed collagen type I.

Albumin secretion by hepatocytes at 24 h, 3 and 7 days on all peptide gels, except RADA at 24 h, was significantly higher than cells on adsorbed collagen type I. Further, addition of RGD2, HB and/or tEGF to the peptide gels significantly improved albumin secretion relative to the non-instructive, unmodified RADA gel. At all time-points, RADA + RGD2 + HB + tEGF showed the highest level of albumin secretion of all the gels. Urea production was significantly higher on all peptide gel formulations, regardless of composition, at all time-points relative to collagen I. Similar toalbumin, inclusion of RGD2, HB, and/or tEGF resulted in a statistically significant improvement in urea production relative to the unmodified RADA gel. Further, normalization of albumin and urea production rates based on total cell numbers for each time point, shows our values are within the range of those typically reported in a variety of other engineered culture systems [38,39].

On peptide gels with the following compositions: RADA + RGD2 + HB, RADA + RGD2 + tEGF, RGD2 + HB + tEGF, albumin and urea secretion by hepatocytes was significantly higher than on adsorbed type I collagen. These phenotypic differences are expected given the ability of the modified peptide gels to engage fibronectin binding-integrins, -syndecans, and/or growth factor receptors, which would not be activated on collagen I. The morphology of the cells may also be linked to these differences given that the hepatocyte area on these gels was significantly lower than adsorbed type I collagen and approximated values reported for hepatocytes in vivo (~2000 μm^2 for RADA + RGD2 + HB + tEGF on day 3, versus ~7000 μm2 for adsorbed collagen I, versus ~2200 μm^2 *in vivo*) and previous studies have shown that maximally spread hepatocytes have a lower metabolism compared to cells with intermediate levels of spreading [15,16,40].

4. Discussion

Biologically inspired self-assembling peptide gels have shown utility in the culture and manipulation of a variety of cell types. By itself, the standard peptide backbone, RADA, does not interact specifically with cells; however, it can be easily functionalized by incorporating short chain peptides with glycine spacers to the C-terminus of the RADA chain [4,20]. Use of peptide gels with such strategies has shown promise in bone, cartilage, neural, and cardiac regeneration [2–5,20,22,41]. Previously self-assembling peptide gels have shown limited success for the culture of primary hepatocytes [22]. However, this is the first report of the combinatorial use of functional motifs capable of engaging integrins, syndecans and growth

factor receptors. Here, we demonstrate that self-assembling peptide gels, by virtue of the modular nature of their modifications, can be functionalized to present adhesive ligands and growth factor signals relevant to a soft tissue microenvironment.

Taking cues from hepatocyte environments *in vivo*, we chose adhesive ligands and a growth factor relevant for the hepatic microenvironment [34]. Hepatocytes express over 200,000 EGF receptors and EGF signaling mediates their morphology, survival, DNA synthesis, and differentiated function. The hepatic sinusoid contains tenascin-C [17], a matrix molecule with EGF-like repeats that are known to activate EGFR in a matricrine fashion [18]. Hence, we created environments that would mimic the matricrine presentation of EGF, anticipating that such presentation would inhibit internalization and downregulation of EGFR, and alter the balance and duration of downstream EGFR signaling pathways compared to soluble EGF. Hepatocytes express three integrin adhesion receptors: α1β1, α5β1 and α9β1 for binding collagen type I, fibronectin and tenascin-C, respectively [42]. We complemented the presentation of EGF in tethered format by including two key cell adhesion peptide domains, the RGD cell-binding domain and the heparin binding from fibronectin to engage α5β1 integrin receptor and its co-receptor, syndecan-4, respectively. The local concentrations of peptide in the gel are estimated to be sufficient for driving receptor dimerization or clustering. The average spacing between two adhesion ligands included at a 1:9 ratio in the gel is estimated to be 8–15 nm, based on the reported dimensions of the nanofibers formed from the gels [43]. These spacings should be sufficient to cluster adhesion receptors [44]. EGF is tethered via a biotin linkage to neutravidin, thus estimates of spacing between EGF are 3–6 nm in the peptide gel, which is sufficient to allow dimerization of EGF receptors [45]. This process used to design modifications of the peptide gel for hepatocellular culture could be undertaken for other soft tissue microenvironments (Fig. 9).

In the liver sinusoid, sheets of hepatocytes are held together by cell–cell contacts while the cell membranes are in direct contact with fibronectin-containing matrix. However, *in vitro*, it has been demonstrated that on insufficiently adhesive substrates, the strength of cell–cell contacts predominate, resulting in spheroids of primary hepatocytes [9]. It has also been shown that supra-physiological cell spreading, such as seen on adsorbed collagen, decreases the metabolic activity of hepatocytes, suggesting that there is an optimal cell morphology associated with maintenance of hepatocyte differentiation [16]. Cell and aggregate morphology have typically been manipulated with combinations of matrix and soluble factors; here, we compared the use of soluble versus surface-tethered EGF as a means to manipulate cell and aggregate morphology and resulting hepatocellular phenotypes.

Not surprisingly, inclusion of adhesion ligands in the peptide gels increased the size of hepatocellular aggregates as well as the average cell area within aggregates (Fig. 1). Hepatocytes seeded in culture as single cells attach and undergo an aggregation process characterized by extension of filipodia, contact with neighbors, and movement toward neighbors to increase cell–cell contact resulting in well-spread monolayers on sufficiently adhesive substrates and rounded spheroids on insufficiently adhesive substrates. In this system, matrix adhesion is mediated by α5β1 and its co-receptor, syndecan-4, the cooperation of which has been shown to be required for optimal cell attachment, spreading, and motility in a variety of cell types [23,46,47]. While it has been reported that soluble syndecan-4 ligands, such as fibronectin, can induce appropriate integrin-syndecan-4 interactions [23,46], we do not believe that soluble factors are responsible for the early stages of attachment and spreading or the morphological differences reported here at day 3. Although unmodified RADA gels can nonspecifically adsorb adhesion proteins present in serum or secreted by cells ([41] and Fig. 3), no serum was present in these cultures and the time scale for cell-secreted fibronectin accumulation (days) appears to preclude its influence on early (up to day 3) events, such as attachment, spreading, and aggregation. Thus, the data indicate that inclusion of minimal

adhesion ligands, RGD2 and HB, greatly increases the average aggregate size and the average cell area of hepatocytes on modified gels with simultaneous ligation of α5β1and syndecan-4 (RADA + RGD2 + HB) showing a greater increase than α5β1 alone (RADA + RGD2). However, hepatocyte morphology is not governed solely by adhesion ligands. Under conditions of moderate-to-high matrix adhesivity, soluble EGF stimulates cell motility [48,49], despite it being anti-adhesive to hepatocytes on poorly adhesive substrata [8]. Hence, it has previously been shown that soluble EGF works in concert with matrix adhesion to facilitate motility and aggregate formation in the early stages of culture. In this report, a dramatic effect on cell morphology was observed for tethered EGF, which increases attachment and spreading of other cell types [21,50], possibly through an N-wasp mediated mechanism leading to local polymerization of actin [51]. Thus, it was expected and shown here that integration of signals from α5β1, syndecan-4, and EGFR (RADA + RGD2 + HB + tEGF) would result in the most extensive attachment and spreading of the peptide gel combinations.

Morphological differences associated with the different adhesion environments also correlated with differences in hepatocyte viability and metabolism. In general, the RADA gel modified with the full compliment of ligands, RGD2, HB, and tEGF, which also supported the largest aggregate and cell areas, was best able to support the desired phenotypes. Hepatocyte cell areas on peptide gels reported here for the most highly modified gel (1950 μmm^2 forRADA + RGD + HB + tEGF at day 3) are similar to the dimensions of hepatocytes *in vivo* (~2200 μm^2) [40] and much less spread than cells on type I collagen (~7000 μm^2) [15,16]. These morphological differences correspond with differences in metabolic function between unmodified and modified peptide gels and adsorbed collagen I that are consistent with other literature reports of poor retention of function in highly spread hepatocytes [16]. They also correspond with viability at early time-points (one and three days), where gels modified with RGD2 and RGD2 + HB show a statistically significant increase in viability. However, after a week in culture, cell viabilities were similar across all modifications. We speculate that accumulation of hepatocyte-secreted soluble fibronectin (Fig. 3) provides a pro-survival adhesion stimulus to cells at later time-points in culture.

The profound differences in cell and aggregate morphology, along with correlated differences in viability and metabolic function, suggested that increased adhesion, and presentation of EGF in tethered rather than soluble format, might alter downstream signaling. ERK is a common signaling pathway activated upon integrin clustering and/or binding of EGF to EGFR [36,52, 53], and integrin-mediated adhesion increases ERK phosphorylation and DNA synthesis in the presence of growth factors in some cell types [36]. Interestingly, in the presence of soluble EGF, activation of ERK1/2 appears only slightly sensitive to addition of the RGD2 or HB domains to the peptide gels (Fig. 5A and B), with overall values much higher than initial isolates (taken at a time point immediately following enzymatic digestion and centrifugation to enrich for hepatocytes) and remaining approximately unchanged from the 48–72 h point. The phosphorylated ERK1/2 values are lower for cells cultured on gels than for those cultured on adsorbed collagen I, a rigid substrate. Strikingly, ERK1/2 shows greatly increased activation levels in cells cultured in the presence of tethered EGF on all peptide gel formulations at both time points, compared to the same adhesive conditions with soluble EGF. These results are intriguing in light of recent reports that enhanced ERK activation in hepatocytes can drive a pro-death phenotype [54–56] while we see it correlating with increased viability. Clearly, ERK1/2 act in a context-dependent fashion and may yield pro-survival signaling in the context of the peptide gel adhesion environment compared to the previous studies where cells were cultured on rigid substrates.

An obvious explanation for the enhanced activation of ERK1/2 in the presence of tethered EGF compared to soluble EGF for cells on peptide gels is retention of EGFR expression via inhibition of internalization and degradation of the EGFR. Examination of EGFR levels under

the different culture conditions (Fig. 7A and B) indicates that EGFR expression is downregulated under all soluble EGF culture conditions, but is maintained at expression levels comparable to freshly isolated cells for all tethered EGF conditions. Because signaling by ligand-bound EGFR can be rapidly shut off by intracellular phosphatase activity, in addition to degradation, we examined levels of pEGFR under all conditions at time points of 0, 48 and 72 h. The fraction of activated EGFR (pEGFR/total EGFR) was slightly higher for the tethered compared to the soluble case at 48 h and dramatically higher at 72 h; taken together with the significantly higher total EGFR levels for the tethered EGF case, pEGFR was very significantly increased in all conditions involving tethered EGF. This increased activity of EGFR is consistent with the increased levels of pERK1/2 observed for these conditions.

The increased ERK1/2 activation for the tethered EGF case could have also arisen from up-regulation of ErbB2, a preferred heterodimerization partner for EGFR and a potent stimulator of several signaling pathways downstream of EGFR. Increased expression of ErbB2 is often a driver of malignant phenotypes in epithelial cells [57]. Primary adult male rat hepatocytes have previously been reported to express undetectably low levels of ErbB2, but upregulate expression dramatically by 48 h in culture on adsorbed collagen I in the presence of insulin and EGF [12]. Dexamethasone, a common additive to serum-free hepatocyte culture media, mitigates the ErbB2 up-regulation and maintains EGFR expression in a highly dose-dependent fashion [11]. Using a different strain of rats (Fischer vs Sprague Dawley) and a different method of quantifying ErbB2 (immunobead assay vs densitometry of Western blots), we found that freshly isolated adult male hepatocytes express low levels of ErbB2 (Fig. 7C). Consistent with the previously published observations of Scheving et al. [11,12,37], total ErbB2 is dramatically upregulated in the first 48–72 h for hepatocytes cultured on rigid collagen I in the presence of insulin and EGF. Our cultures contain an intermediate concentration of dexamethasone (100 nM) hence the level of up-regulation is consistent with the previous report [11]. The increased ErbB2 expression was accompanied by a high degree of ErbB2 phosphorylation (Fig. 6).

Surprisingly, given the differences in morphology and function described earlier, the up-regulation and phosphorylation of ErbB2 in hepatocytes cultured on peptide gels in the presence of soluble EGF almost precisely mirrored that of cells cultured on rigid collagen I in the presence of soluble EGF (Figs. 6 and 7). More surprisingly, tethered EGF suppressed up-regulation and reduced phosphorylation of ErbB2 entirely under all conditions (Figs. 6 and 7). We infer from these results that presentation of EGF tethered via neutravidin to the peptide gels is sufficient to allow homodimerization of the EGFR, although we do not rule out release of autocrine EGFR ligands as a means of homodimerization as hepatocytes make abundant TGF-α [27]. It has also been reported that EGFR can be activated by α5β1 through a Src-dependent mechanism [58], and it is thus possible that juxtapositioning of the ligand-bound EGFR to ligand-bound integrins contributes to activation of EGFR [33]. Further studies are underway to explore these possibilities.

Finally, the most unexpected result in this study was the observed pattern of DNA synthesis on peptide gels. Under specific conditions, primary adult rat hepatocytes in culture can be stimulated to enter the cell cycle and synthesize DNA – those conditions typically include strong cell adhesion, extensive spreading, low cell density (<50,000 cells/cm^2), stiff substratum, presence of insulin, and EGF signaling with prolonged downstream activation of ERK1/2 [12,13,15]. However, hepatocytes *in vivo* are capable of entering and continuing through the cell cycle during liver regeneration, even though the liver is a relatively soft microenvironment where cells are densely packed, and are not extensively spread. We quantified DNA synthesis at time-points commonly associated with hepatocyte DNA synthesis in primary culture (between 48 and 72 h) using direct counting of BrdU-labeled nuclei. For cells cultured on rigid collagen I, the amount of DNA synthesis (Fig. 4) is within an expected range for this condition given the relatively high cell densities used (65,000 cells/cm^2).

However, cells on peptide gels did not exhibit any measurable DNA synthesis in the presence of soluble EGF for any of the adhesive conditions (Fig. 4). In the presence of tethered EGF, only peptide gels modified with RGD2, HB, and tethered EGF, from 48 to 72 h, promoted DNA synthesis by ~40% of hepatocytes (compared to ~50% for hepatocytes on collagen I during the same time period). This observation of hepatocyte DNA synthesis on a substrate approximating physiological stiffness is notable. While a previous study has illustrated that primary hepatocytes can be induced to synthesize DNA on soft collagen substrates by inhibiting PKA activity [15], mimicking PKA levels on stiff collagen substrates, we show here that the soft modified peptide gel can elicit the same response in the absence of specific pathway inhibitor. The mechanism responsible for DNA synthesis on peptide gels is currently unknown, but it is unlikely it is mediated by ERK1/2 as the activation levels of ERK1/2 are comparable for all tethered EGF substrates at all time-points studied. Additional pathways downstream of EGFR (including JNK, PKC, STAT, PLCγ) and integrins (including JNK, ROCK, AKT, PAK) are candidates for the regulation of behavior and the subject of ongoing studies.

This pattern of DNA synthesis is also remarkable because previously, DNA synthesis by cells on collagen I in the presence of soluble EGF has been linked to increased expression and phosphorylation of ErbB2. Comparing cells on peptide gels (a soft substrate with mechanical properties similar to normal liver) versus collagen I (a rigid substrate) in the presence of soluble EGF shows an increase in ErbB2 expression under both culture conditions relative to freshly isolated hepatocytes. However, cells on peptide gels exhibit lower levels of ERK1/2 and ErbB2 activation with soluble EGF compared to cells cultured on collagen. While this would appear to explain the lack of DNA synthesis on the peptide gels with soluble EGF, results with tethered EGF indicate a more complicated scenario. The only condition on which DNA synthesis is observed on the gels, RADA + RGD2+HB + tEGF, corresponds to ERK1/2 activation in the absence of ErbB2 up-regulation or phosphorylation (levels are comparable to fresh isolates). It would appear that, unlike cultures with soluble EGF on collagen I or peptide gels, DNA synthesis is stimulated via tethered EGF activating EGFR and ERK1/2 without altering levels of EGFR or ErbB2. While there were no differences observed in the levels of phosphorylation of EGFR, ErbB2 or ERK1/2 between gels with different adhesion ligands, DNA synthesis was only observed in the presence of RGD2 and HB, indicating that integrin and syndecan signaling are critical. In summary, RADA + RGD2 + HB + tEGF stimulated hepatocyte DNA synthesis by increasing activation of EGFR and ERK1/2, yet maintaining EGFR, ErbB2, and the phosphorylated ErbB2 at levels found in fresh isolates.

These discoveries set the stage for additional investigations of how the mode of growth factor presentation, in concert with adhesion receptor engagement, regulates hepatocellular survival and apoptosis under conditions of cell stress, such as stimulation with inflammatory cytokines or infection with a virus. When exposed to certain inflammatory cytokine combinations, hepatocytes initiate a set of self-antagonizing autocrine loops involving EGFR receptor ligands along with IL1-α, IL1-β, and IL1-ra [27]. These autocrine loops work in concert with exogenous EGFR ligands (and other factors) in non-linear ways to dictate cell phenotypic responses (life or death). We speculate that the new observations here regarding hepatocellular responses to stimulation by tethered EGF may illuminate additional critical facets of hepatocellular biology in the future.

5. Conclusion

The results described in this report strengthen the accumulating evidence that matrix mechanical properties and composition co-regulate cell functions ranging from survival to differentiation by demonstrating the phenotypic and signaling responses to a panel of stimuli with systematic variation in properties. The results also add an extra dimension to this conceptual view, in that the mode of growth factor presentation (soluble vs. tethered) is a critical

determinant of phenotypic outcomes that depend on synergistic stimulation of adhesion and growth factor receptors, perhaps through regulation of growth factor receptor trafficking. The system employed in this work may find use in investigations of cell types from other soft tissues, where interactions between fibronectin receptors and EGFR are implicated in cellular responses.

Supplementary Material

Refer to Web version on PubMed Central for supplementary material.

Acknowledgments

We thank Lisa Spirio (3DM, Cambridge, MA) for generously providing RADA-16-I peptide, biotinylated RADA-16-I peptide and RGD functionalized peptide gel samples. We are thankful to Rachel Pothier (Griffith lab) for provision of primary hepatocytes. We also thank Prof. Richard Lee and Prof. Shuguang Zhang for helpful discussions. We thank Frank Li and Tracey Allen for help with some experiments and data analysis of DNA synthesis, respectively. L. Alvarez acknowledges the generous support of the US Army and the Fannie and John Hertz Foundation for a graduate fellowship. This research was supported by NIBIB (R01EB003805); NIDCR (R01DE019523); NIEHS (through the MIT Center for Environmenal Health Sciences P30ES002109, and R01ES015241) and the US Armed Forces Institute for Regenerative Medicine. We also thank the National Science Foundation, Directorate for Biology and MIT Biological Engineering-Research Experience for Undergraduates (REU) Program for an undergraduate internship to M.L.

References

[1]. Griffith LG, Swartz MA. Capturing complex 3D tissue physiology in vitro. Nat Rev Mol Cell Biol 2006;7(3):211–24. [PubMed: 16496023]

[2]. Davis ME, Hsieh PC, Takahashi T, Song Q, Zhang S, Kamm RD, et al. Local myocardial insulin-like growth factor 1 (IGF-1) delivery with biotinylated peptide nanofibers improves cell therapy for myocardial infarction. Proc Natl Acad Sci U S A 2006;103(21):8155–60. [PubMed: 16698918]

[3]. Ellis-Behnke RG, Liang YX, You SW, Tay DK, Zhang S, So KF, et al. Nano neuro knitting: peptide nanofiber scaffold for brain repair and axon regeneration with functional return of vision. Proc Natl Acad Sci U S A 2006;103(13):5054–9. [PubMed: 16549776]

[4]. Horii A, Wang X, Gelain F, Zhang S. Biological designer self-assembling peptide nanofiber scaffolds significantly enhance osteoblast proliferation, differentiation and 3-D migration. PloS One 2007;2 (2):e190, 1–9. [PubMed: 17285144]

[5]. Kisiday J, Jin M, Kurz B, Hung H, Semino C, Zhang S, et al. Self-assembling peptide hydrogel fosters chondrocyte extracellular matrix production and cell division: implications for cartilage tissue repair. Proc Natl Acad Sci U S A 2002;99(15):9996–10001. [PubMed: 12119393]

[6]. Padin-Iruegas ME, Misao Y, Davis ME, Segers VF, Esposito G, Tokunou T, et al. Cardiac progenitor cells and biotinylated insulin-like growth factor-1 nanofibers improve endogenous and exogenous myocardial regeneration after infarction. Circulation 2009;120(10):876–87. [PubMed: 19704095]

[7]. Natarajan A, Wagner B, Sibilia M. The EGF receptor is required for efficient liver regeneration. Proc Natl Acad Sci U S A 2007;104(43):17081–6. [PubMed: 17940036]

[8]. Kuhl PR, Griffith-Cima LG. Tethered epidermal growth factor as a paradigm for growth factor-induced stimulation from the solid phase. Nat Med 1996;2(9):1022–7. [PubMed: 8782461]

[9]. Powers MJ, Rodriguez RE, Griffith LG. Cell-substratum adhesion strength as a determinant of hepatocyte aggregate morphology. Biotechnol Bioeng 1997;53(4):415–26. [PubMed: 18634032]

[10]. McClelland R, Wauthier E, Uronis J, Reid L. Gradients in the liver's extracellular matrix chemistry from periportal to pericentral zones: influence on human hepatic progenitors. Tissue Eng Part A 2008;14(1):59–70. [PubMed: 18333805]

[11]. Scheving LA, Buchanan R, Krause MA, Zhang X, Stevenson MC, Russell WE. Dexamethasone modulates ErbB tyrosine kinase expression and signaling through multiple and redundant mechanisms in cultured rat hepatocytes. Am J Physiol 2007;293(3):G552–9.

[12]. Scheving LA, Zhang L, Stevenson MC, Kwak ES, Russell WE. The emergence of ErbB2 expression in cultured rat hepatocytes correlates with enhanced and diversified EGF-mediated signaling. Am J Physiol 2006;291(1):G16–25.

[13]. Tomomura A, Sawada N, Sattler GL, Kleinman HK, Pitot HC. The control of DNA synthesis in primary cultures of hepatocytes from adult and young rats: interactions of extracellular matrix components, epidermal growth factor, and the cell cycle. J Cell Physiol 1987;130(2):221–7. [PubMed: 3493248]

[14]. Reddy CC, Niyogi SK, Wells A, Wiley HS, Lauffenburger DA. Engineering epidermal growth factor for enhanced mitogenic potency. Nat Biotechnol 1996;14(13):1696–9. [PubMed: 9634854]

[15]. Fassett J, Tobolt D, Hansen LK. Type I collagen structure regulates cell morphology and EGF signaling in primary rat hepatocytes through cAMP-dependent protein kinase A. Mol Biol Cell 2006;17(1):345–56. [PubMed: 16251347]

[16]. Mooney D, Hansen L, Vacanti J, Langer R, Farmer S, Ingber D. Switching from differentiation to growth in hepatocytes: control by extracellular matrix. J Cell Physiol 1992;151(3):497–505. [PubMed: 1295898]

[17]. Scoazec JY, Flejou JF, D'Errico A, Couvelard A, Kozyraki R, Fiorentino M, et al. Focal nodular hyperplasia of the liver: composition of the extracellular matrix and expression of cell–cell and cell–matrix adhesion molecules. Hum Pathol 1995;26(10):1114–25. [PubMed: 7557945]

[18]. Swindle CS, Tran KT, Johnson TD, Banerjee P, Mayes AM, Griffith L, et al. Epidermal growth factor (EGF)-like repeats of human tenascin-C as ligands for EGF receptor. J Cell Biol 2001;154 (2):459–68. [PubMed: 11470832]

[19]. Platt MO, Roman AJ, Wells A, Lauffenburger DA, Griffith LG. Sustained epidermal growth factor receptor levels and activation by tethered ligand binding enhances osteogenic differentiation of multi-potent marrow stromal cells. J Cell Physiol 2009;221(2):306–17. [PubMed: 19544388]

[20]. Genove E, Shen C, Zhang S, Semino CE. The effect of functionalized self-assembling peptide scaffolds on human aortic endothelial cell function. Biomaterials 2005;26(16):3341–51. [PubMed: 15603830]

[21]. Fan VH, Tamama K, Au A, Littrell R, Richardson LB, Wright JW, et al. Tethered epidermal growth factor provides a survival advantage to mesenchymal stem cells. Stem Cells 2007;25(5):1241–51. [PubMed: 17234993]

[22]. Genove E, Schmitmeier S, Sala A, Borros S, Bader A, Griffith LG, et al. Functionalized self-assembling peptide hydrogel enhance maintenance of hepatocyte activity in vitro. J Cell Mol Med. 2009 doi:10.1111/j.1582–4934.2009.00970.x. Epub online.

[23]. Woods A, McCarthy JB, Furcht LT, Couchman JR. A synthetic peptide from the COOH-terminal heparin-binding domain of fibronectin promotes focal adhesion formation. Mol Biol Cell 1993;4 (6):605–13. [PubMed: 8374170]

[24]. Martin A, Baker TA, Sauer RT. Rebuilt AAA + motors reveal operating principles for ATP-fuelled machines. Nature 2005;437(7062):1115–20. [PubMed: 16237435]

[25]. Moll JR, Ruvinov SB, Pastan I, Vinson C. Designed heterodimerizing leucine zippers with a ranger of pIs and stabilities up to 10(−15) m. Protein Sci 2001;10(3):649–55. [PubMed: 11344333]

[26]. Shen W, Zhang K, Kornfield JA, Tirrell DA. Tuning the erosion rate of artificial protein hydrogels through control of network topology. Nat Mater 2006;5(2):153–8. [PubMed: 16444261]

[27]. Cosgrove BD, Cheng C, Pritchard JR, Stolz DB, Lauffenburger DA, Griffith LG. An inducible autocrine cascade regulates rat hepatocyte proliferation and apoptosis responses to tumor necrosis factor-alpha. Hepatology 2008;48(1):276–88. [PubMed: 18536058]

[28]. Stamatoglou SC, Enrich C, Manson MM, Hughes RC. Temporal changes in the expression and distribution of adhesion molecules during liver development and regeneration. J Cell Biol 1992;116 (6):1507–15. [PubMed: 1531833]

[29]. Stamatoglou SC, Hughes RC. Dynamic interactions of hepatocytes with fibronectin substrata: temporal and spatial changes in the distribution of adhesive contacts fibronectin receptors, and actin filaments. Exp Cell Res 1992;198(1):179–82. [PubMed: 1530751]

[30]. Stamatoglou SC, Hughes RC, Lindahl U. Rat hepatocytes in serum-free primary culture elaborate an extensive extracellular matrix containing fibrin and fibronectin. J Cell Biol 1987;105(5):2417–25. [PubMed: 3316251]

[31]. Glading A, Lauffenburger DA, Wells A. Cutting to the chase: calpain proteases in cell motility. Trends Cell Biol 2002;12(1):46–54. [PubMed: 11854009]

[32]. Petersen B, Yee CJ, Bowen W, Zarnegar R, Michalopoulos GK. Distinct morphological and mito-inhibitory effects induced by TGF-beta 1, HGF and EGF on mouse, rat and human hepatocytes. Cell Biol Toxicol 1994;10(4):219–30. [PubMed: 7895151]

[33]. Streuli CH, Akhtar N. Signal co-operation between integrins and other receptor systems. Biochem J 2009;418(3):491–506. [PubMed: 19228122]

[34]. Martinez-Hernandez A, Amenta PS. The hepatic extracellular matrix. I. Components and distribution in normal liver. Virchows Archiv 1993;423(1):1–11. [PubMed: 8212529]

[35]. Loyer P, Cariou S, Glaise D, Bilodeau M, Baffet G, Guguen-Guillouzo C. Growth factor dependence of progression through G1 and S phases of adult rat hepatocytes in vitro. Evidence of a mitogen restriction point in mid-late G1. J Biol Chem 1996;271(19):11484–92. [PubMed: 8626707]

[36]. Asthagiri AR, Reinhart CA, Horwitz AF, Lauffenburger DA. The role of transient ERK2 signals in fibronectin- and insulin-mediated DNA synthesis. J Cell Sci 2000;113(24):4499–510. [PubMed: 11082043]

[37]. Scheving LA, Stevenson MC, Zhang X, Russell WE. Cultured rat hepatocytes upregulate Akt and ERK in an ErbB-2-dependent manner. Am J Physiol 2008;295(2):G322–31.

[38]. Sivaraman A, Leach JK, Townsend S, Iida T, Hogan BJ, Stolz DB, et al. A microscale in vitro physiological model of the liver: predictive screens for drug metabolism and enzyme induction. Curr Drug Metab 2005;6(6):569–91. [PubMed: 16379670]

[39]. Miranda JP, Leite SB, Muller-Vieira U, Rodrigues A, Carrondo MJ, Alves PM. Towards an extended functional hepatocyte in vitro culture. Tissue Eng Part C Methods 2009;15(2):157–67. [PubMed: 19072051]

[40]. Blendis LM, Orrego H, Crossley IR, Blake JE, Medline A, Isreal Y. The role of hepatocyte enlargement in hepatic pressure in cirrhotic and noncirrhotic alcoholic liver disease. Hepatology 1982;2(5):539–46. [PubMed: 7118067]

[41]. Sieminski AL, Was AS, Kim G, Gong H, Kamm RD. The stiffness of three-dimensional ionic self-assembling peptide gels affects the extent of capillary-like network formation. Cell Biochem Biophys 2007;49(2):73–83. [PubMed: 17906362]

[42]. Ramadori G, Schwogler S, Veit T, Rieder H, Chiquet-Ehrismann R, Mackie EJ, et al. Tenascin gene expression in rat liver and in rat liver cells. In vivo and in vitro studies. Virchows Arch B Cell Pathol Incl Mol Pathol 1991;60(3):145–53. [PubMed: 1715623]

[43]. Park J, Kahng B, Kamm RD, Hwang W. Atomistic simulation approach to a continuum description of self-assembled beta-sheet filaments. Biophys J 2006;90(7):2510–24. [PubMed: 16415051]

[44]. Kuhlman W, Taniguchi I, Griffith LG, Mayes AM. Interplay between PEO tether length and ligand spacing governs cell spreading on RGD-modified PMMA-g-PEO comb copolymers. Biomacromolecules 2007;8(10):3206–13. [PubMed: 17877394]

[45]. Ogiso H, Ishitani R, Nureki O, Fukai S, Yamanaka M, Kim JH, et al. Crystal structure of the complex of human epidermal growth factor and receptor extracellular domains. Cell 2002;110(6):775–87. [PubMed: 12297050]

[46]. Bass MD, Morgan MR, Humphries MJ. Integrins and syndecan-4 make distinct, but critical, contributions to adhesion contact formation. Soft Matter 2007;3(3):372–6. [PubMed: 19458789]

[47]. Midwood KS, Schwarzbauer JE. Tenascin-C modulates matrix contraction via focal adhesion kinase- and Rho-mediated signaling pathways. Mol Biol Cell 2002;13(10):3601–13. [PubMed: 12388760]

[48]. Cabodi S, Moro L, Bergatto E, Boeri Erba E, Di Stefano P, Turco E, et al. Integrin regulation of epidermal growth factor (EGF) receptor and of EGF-dependent responses. Biochem Soc Trans 2004;32(3):438–42. [PubMed: 15157155]

[49]. Maheshwari G, Brown G, Lauffenburger DA, Wells A, Griffith LG. Cell adhesion and motility depend on nanoscale RGD clustering. J Cell Sci 2000;113(10):1677–86. [PubMed: 10769199]

[50]. Marcantonio NA, Boehm CA, Rozic RJ, Au A, Wells A, Muschler GF, et al. The influence of tethered epidermal growth factor on connective tissue progenitor colony formation. Biomaterials 2009;30(27):4629–38. [PubMed: 19540579]

[51]. Kempiak SJ, Yamaguchi H, Sarmiento C, Sidani M, Ghosh M, Eddy RJ, et al. A neural Wiskott-Aldrich Syndrome protein-mediated pathway for localized activation of actin polymerization that is regulated by cortactin. J Biol Chem 2005;280(7):5836–42. [PubMed: 15579908]

[52]. Asthagiri AR, Nelson CM, Horwitz AF, Lauffenburger DA. Quantitative relationship among integrin-ligand binding, adhesion, and signaling via focal adhesion kinase and extracellular signal-regulated kinase 2. J Biol Chem 1999;274(38):27119–27. [PubMed: 10480927]

[53]. Cybulsky AV, McTavish AJ, Cyr MD. Extracellular matrix modulates epidermal growth factor receptor activation in rat glomerular epithelial cells. J Clin Invest 1994;94(1):68–78. [PubMed: 8040293]

[54]. Cosgrove BD, King BM, Hasan MA, Alexopoulos LG, Farazi PA, Hendriks BS, et al. Synergistic drug-cytokine induction of hepatocellular death as an in vitro approach for the study of inflammation-associated idiosyncratic drug hepatotoxicity. Toxicol Appl Pharmacol 2009;237(3):317–30. [PubMed: 19362101]

[55]. Fremin C, Bessard A, Ezan F, Gailhouste L, Regeard M, Le Seyec J, et al. Multiple division cycles and long-term survival of hepatocytes are distinctly regulated by extracellular signal-regulated kinases ERK1 and ERK2. Hepatology 2009;49(3):930–9. [PubMed: 19177593]

[56]. Fremin C, Ezan F, Boisselier P, Bessard A, Pages G, Pouyssegur J, et al. ERK2 but not ERK1 plays a key role in hepatocyte replication: an RNAi-mediated ERK2 knockdown approach in wild-type and ERK1 null hepatocytes. Hepatology 2007;45(4):1035–45. [PubMed: 17393467]

[57]. Lohrisch C, Piccart M. An overview of HER2. Semin Oncol 2001;28(6 Suppl.18):3–11. [PubMed: 11774200]

[58]. Kuwada SK, Li X. Integrin alpha5/beta1 mediates fibronectin-dependent epithelial cell proliferation through epidermal growth factor receptor activation. Mol Biol Cell 2000;11(7):2485–96. [PubMed: 10888683]

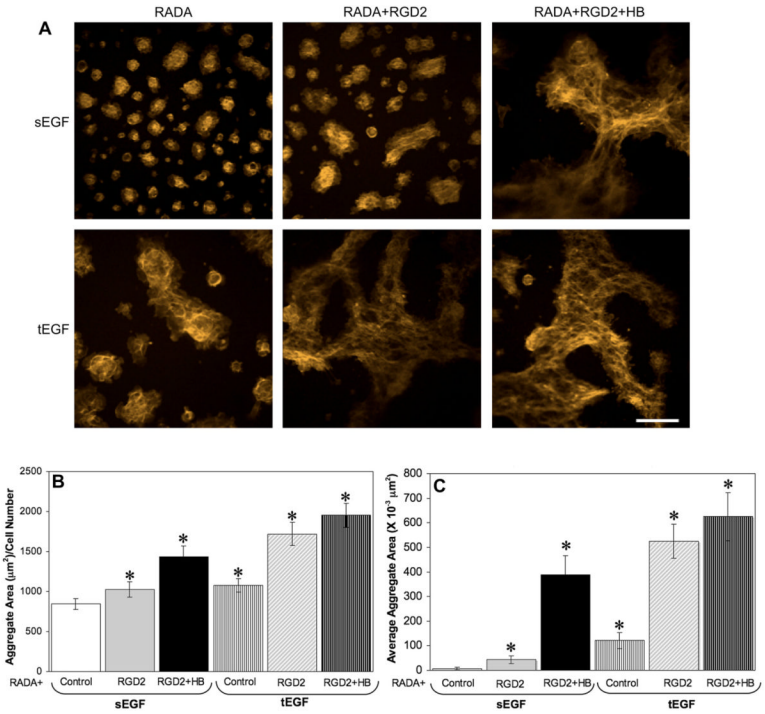

Fig. 1.

Self-assembling peptide gels functionalized with the cell-binding domain and heparin binding domain of fibronectin and tethered EGF influence hepatocyte morphology and adhesion. A) Representative fluorescent actin cytoskeleton images (5× objective) for hepatocytes on RADA, RADA + RGD2, RADA + RGD2 + HB peptide gels with soluble EGF or tEGF, 3 days after initial seeding (Scale bar = 400 μm). B) Quantification of average cell aggregate area at day 3 on peptide gels, and C) Quantification of average cell area at day 3 on peptide gels expressed as ratio of total aggregate area and total nuclei counted. Fluorescent actin and DAPI images of each peptide gel sample (seeded at 100,000 cells/cm^2) were taken in 4–5 fields at each time point. * indicates statistically significant difference from RADA with soluble EGF, $p < 0.05$, $n > 3$.

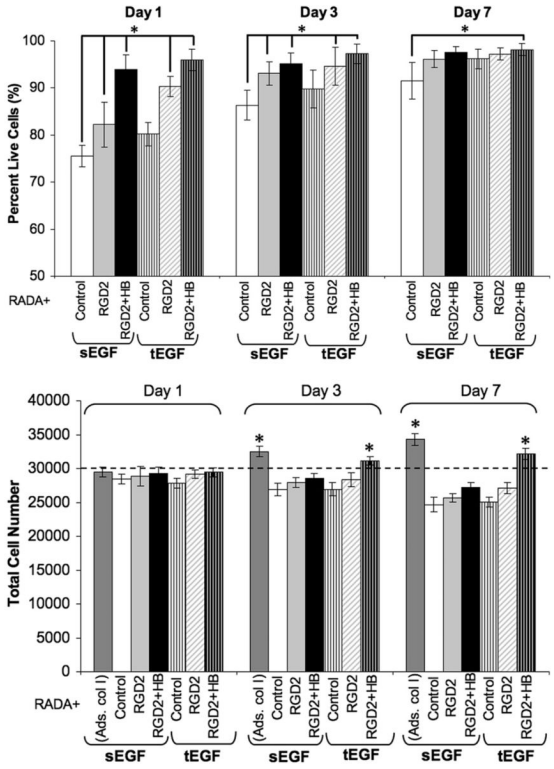

Fig. 2.

Adhesion ligands and tethered growth factor modulate hepatocyte viability on self-assembling peptides for seven days in culture. A) Quantification of cell viability expressed as percentage live cells as a function of gel composition, B) Total cell numbers as a function of time in culture. Hepatocytes on RADA, RADA + RGD2 RADA + RGD2 + HB peptide gels with soluble EGF or tEGF (seeded at 65,000 cells/cm^2) were stained with EtBr and DAPI at each time point. Images representing four random fields were taken on each peptide gel sample. Cell viability was defined as the fraction of non-EtBr stained cells in the field. Except adsorbed collagen I (ads. col I), all peptide gels contained RADA. * indicates statistically significant difference from RADA with soluble EGF at a specific day, $p < 0.05$, $n > 3$.

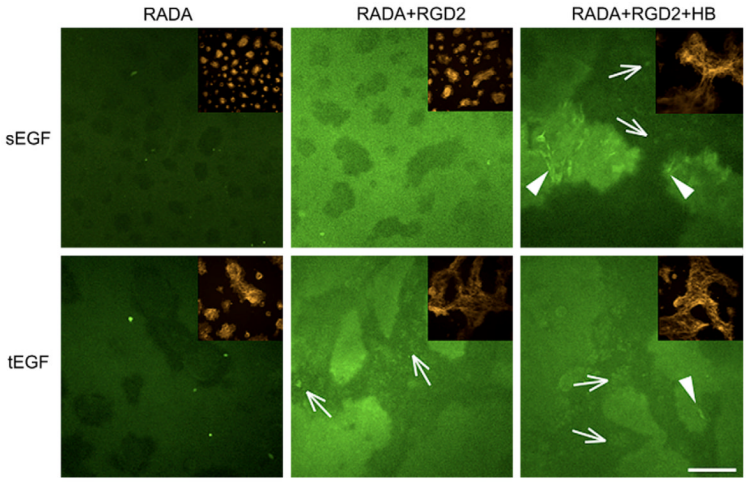

Fig. 3.

Inclusion of adhesion ligands and tethered growth factor instruct hepatocyte to secrete and accumulate matrix after 3 days in culture on self-assembling peptide gels. Representative images of fibronectin and actin (inset) on RADA, RADA + RGD2, RADA + RGD2 + HB peptide gels with soluble EGF or tEGF 3 days after initial seeding at 100,000 cells/cm^2 (Scale bar = 400 mm, 5× objective). Cells were fixed, permeabilized and stained with anti-rat fibronectin and four random fields were imaged on each peptide gel sample. Arrows indicate intracellular staining for fibronectin and arrowheads point to extracellular fibrils of fibronectin.

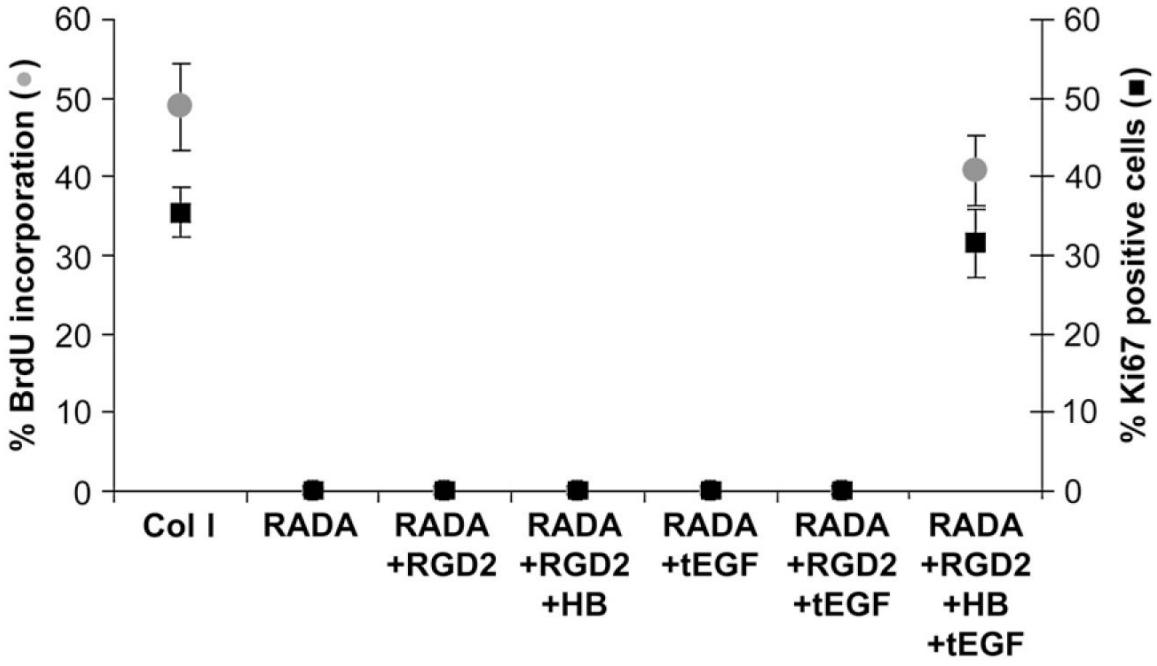

Fig. 4.

Primary hepatocytes require presence of RGD, HB and tEGF on peptide gels in order to synthesize DNA. Quantification of DNA synthesis by BrdU incorporation and active cell cycle marker Ki67. Hepatocytes (seeded at 65,000 cells/cm^2) were cultured on RADA, RADA + RGD2 and RADA + RGD2 + HB peptide gels with soluble EGF or tEGF and adsorbed collagen I (Col I). DNA synthesis was quantified by immunofluorescence staining as the percentage of total nuclei incorporating BrdU (48–72 h) or as the percentage of total nuclei staining positive for Ki67 (at 48 h). We observed no DNA synthesis at any time point on other peptide gel (RADA, RADA + RGD2, RADA + RGD2 + HB all with soluble EGF and RADA + tEGF, RADA + RGD2 + tEGF).

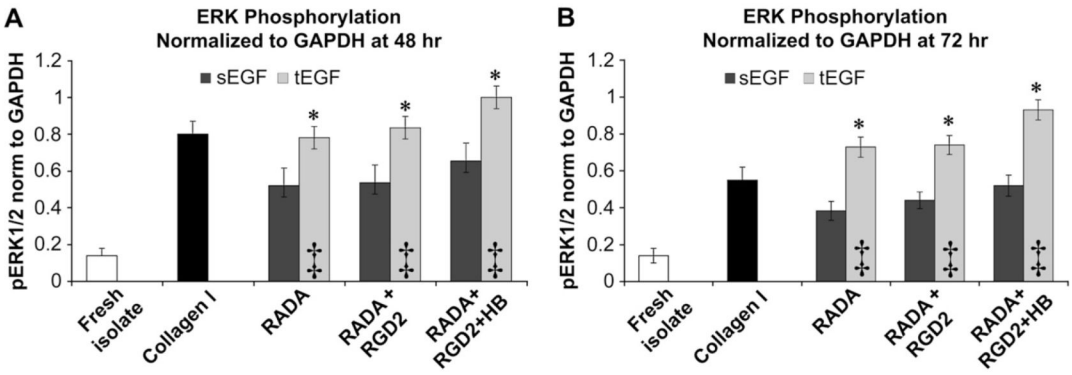

Fig. 5.

Addition of tEGF to peptide gels with varying adhesion ligands leads to sustained ERK phosphorylation in hepatocytes. ERK phosphorylation (normalized to GAPDH) at A) 48 h, B) 72 h. Hepatocytes were cultured on RADA, RADA + RGD2 and RADA + RGD2 + HB peptide gels with soluble EGF or tEGF or tEGF (seeded at 100,000 cells/cm^2). Lysates were made after defined time-points and pERK levels were quantified by immunoprecipitation. * indicates statistically significant difference from RADA with soluble EGF, ‡ indicates statistically significant difference between soluble and tethered for a particular peptide gel composition, $p < 0.05$, $n > 2$.

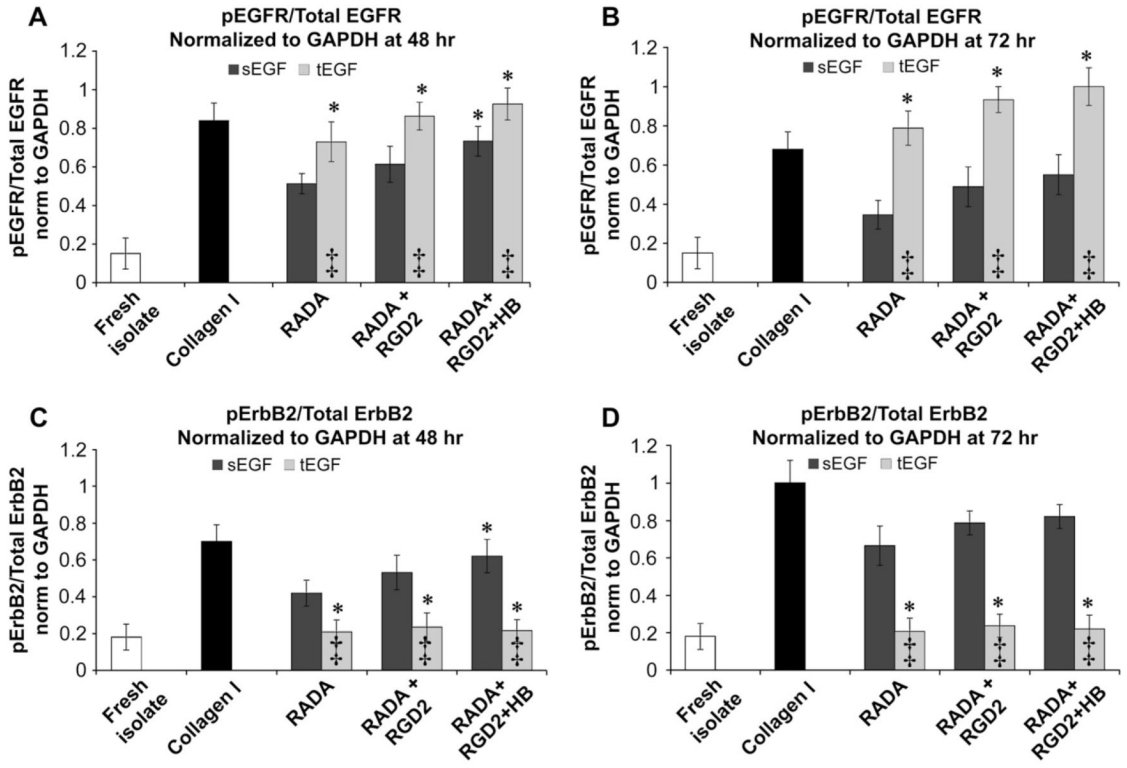

Fig. 6.

Tethered EGF stimulates sustained EGFR phosphorylation and downregulates ErBB2 phosphorylation in hepatocytes on peptide gels. EGFR phosphorylation (normalized to total EGFR and GAPDH) at A) 48 h, B) 72 h, and ErbB2 phosphorylation (normalized to total ErbB2 and GAPDH) at C) 48 h, D) 72 h. Hepatocytes were cultured on peptide gels with soluble EGF or tEGF or tEGF (seeded at 100,000 cells/cm^2). Lysates were made after defined time-points and pEGFR levels were quantified by immunoprecipitation. * indicates statistically significant difference from RADA with soluble EGF, ‡ indicates statistically significant difference between soluble and tethered for a particular peptide gel composition, $p < 0.05$, $n > 2$.

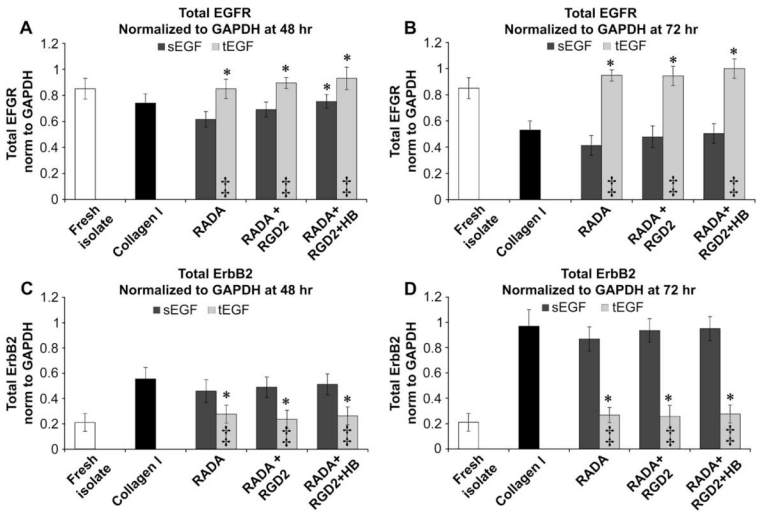

Fig. 7.

Tethered EGF maintains total EGFR and downregulates ErbB2 receptor levels on peptide gels. Total EGFR (normalized to GAPDH) at A) 48 h, B) 72 h, and total ErbB2 (normalized to GAPDH) at C) 48 h, D) 72 h. Hepatocytes were cultured on peptide gels with soluble EGF or tEGF or tEGF (seeded at 100,000 cells/cm^2). Lysates were made after defined time-points and pEGFR levels were quantified by immunoprecipitation. * indicates statistically significant difference from RADA with soluble EGF, ‡ indicates statistically significant difference between soluble and tethered for a particular peptide gel composition, $p < 0.05$, $n > 2$.

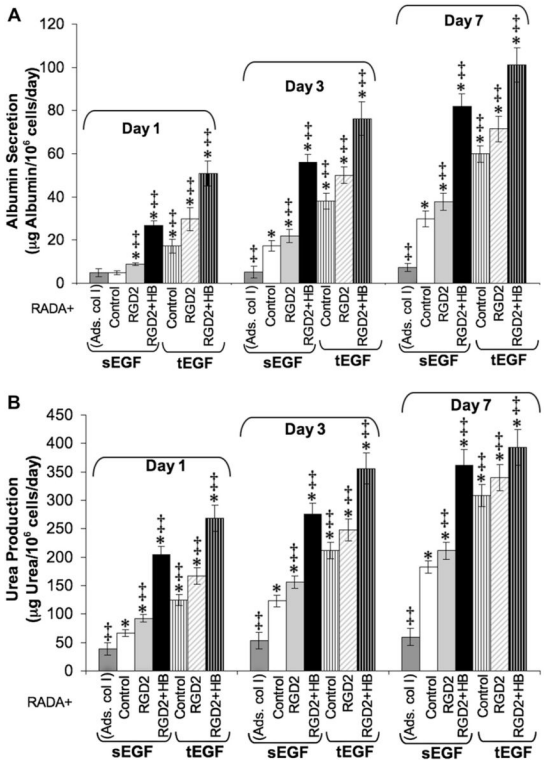

Fig. 8.

Maintenance of metabolic function improves with functionalization of peptide gels with adhesion ligands and growth factor tethering. A) Albumin secretion, B) Urea production. Conditioned media from hepatocyte cultures on peptide gels and adsorbed collagen I (seeded at 100,000 cells/cm^2) were collected, and urea and albumin were quantified using standard assay kits. Culture medium was replaced 48 h prior to collection on the indicated days. Samples, standards and controls were tested in duplicates. ‡ indicates statistically significant difference from RADA, $p < 0.05$, $n > 3$, Except adsorbed collagen I (ads. col I), all peptide gels contained RADA. * indicates statistically significant difference from adsorbed collagen I, $p < 0.05$, $n > 3$.

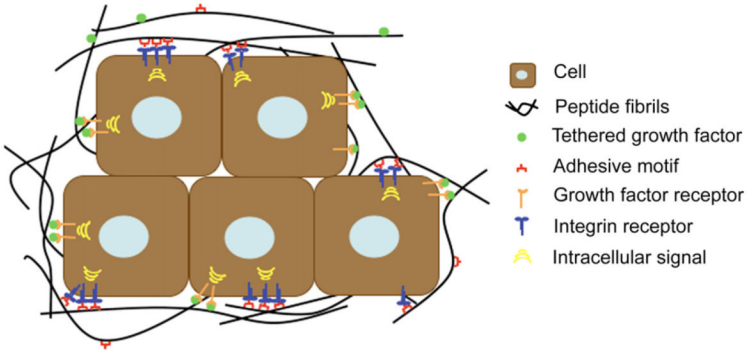

Fig. 9.

Self-assembling peptide gels modified with adhesive ligands and tethered growth factors may provide adequate microenvironment to various cell types. The peptide backbone can be modified with a variety of adhesive modifications suitable to the integrin repertoire of any cell type. Further, inclusion of a biotin modification on the peptide backbone allows any biotinylated growth factor to be tethered to the gel. Given the stiffness of the peptide gels are physiological for many tissues, these gels can be modified to suit a wide array of cell types forming a chemically and mechanically controlled microenvironment.

Table 1

Self-assembling peptide gel composition and notation

Composition of the self-assembling peptide gel	Ratio of components	Notation in this report
RADA + Biotinylated RADA	9:1	RADA
RADA + Biotinylated RADA + RGD2 functionalized RADA	8:1:1	RADA + RGD2
RADA + Biotinylated RADA + RGD2 functionalized RADA + Heparin binding functionalized RADA	7:1:1:1	RADA + RGD2 + HB
RADA + Biotinylated RADA + tethered EGF	9:1	RADA + tEGF
RADA + Biotinylated RADA + RGD2 functionalized RADA + tethered EGF	8:1:1	RADA + RGD2 + tEGF
RADA + Biotinylated RADA + RGD2 functionalized RADA + Heparin binding functionalized RADA tethered EGF	7:1:1:1	RADA + RGD2 + HB + tEGF